



**HAL**  
open science

## Stability of a pinned magnetic domain wall as a function of its internal configuration

François Montaigne, Amandine Duluard, Joel Briones, Daniel Lacour, Michel Hehn, J. R. Childress

► **To cite this version:**

François Montaigne, Amandine Duluard, Joel Briones, Daniel Lacour, Michel Hehn, et al.. Stability of a pinned magnetic domain wall as a function of its internal configuration. *Journal of Applied Physics*, 2015, 117 (2), pp.023909. 10.1063/1.4905245 . hal-01284013

**HAL Id: hal-01284013**

**<https://hal.science/hal-01284013v1>**


Submitted on 21 Aug 2024

**HAL** is a multi-disciplinary open access archive for the deposit and dissemination of scientific research documents, whether they are published or not. The documents may come from teaching and research institutions in France or abroad, or from public or private research centers.

L'archive ouverte pluridisciplinaire **HAL**, est destinée au dépôt et à la diffusion de documents scientifiques de niveau recherche, publiés ou non, émanant des établissements d'enseignement et de recherche français ou étrangers, des laboratoires publics ou privés.

RESEARCH ARTICLE | JANUARY 14 2015

# Stability of a pinned magnetic domain wall as a function of its internal configuration


F. Montaigne ; A. Duluard; J. Briones; D. Lacour; M. Hehn; J. R. Childress


 Check for updates


*J. Appl. Phys.* 117, 023909 (2015)


<https://doi.org/10.1063/1.4905245>




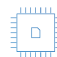
 Nanotechnology & Materials Science


 Optics & Photonics

 Impedance Analysis

 Scanning Probe Microscopy


 Sensors

 Failure Analysis & Semiconductors



Unlock the Full Spectrum.  
From DC to 8.5 GHz.  
Your Application. Measured.

[Find out more](#)



# Stability of a pinned magnetic domain wall as a function of its internal configuration

F. Montaigne,<sup>1</sup> A. Duluard,<sup>1</sup> J. Briones,<sup>1</sup> D. Lacour,<sup>1</sup> M. Hehn,<sup>1</sup> and J. R. Childress<sup>2</sup>

<sup>1</sup>*Institut Jean Lamour, Université de Lorraine, CNRS, BP 70239, F-54506 Vandoeuvre lès Nancy, France*

<sup>2</sup>*HGST San Jose Research Center, 3403 Yerba Buena Rd, San Jose, California 95135, USA*

(Received 7 September 2014; accepted 17 December 2014; published online 14 January 2015)

It is shown that there are many stable configurations for a domain wall pinned by a notch along a magnetic stripe. The stability of several of these configurations is investigated numerically as a function of the thickness of the magnetic film. The depinning mechanism depends on the structure of the domain wall and on the thickness of the magnetic film. In the case of a spin-valve structure, it appears that the stray fields emerging from the hard layer at the notch location influence the stability of the micromagnetic configuration. Different depinning mechanisms are thus observed for the same film thickness depending on the magnetization orientation of the propagating domain. This conclusion qualitatively explains experimental magnetoresistance measurements. © 2015 AIP Publishing LLC. [<http://dx.doi.org/10.1063/1.4905245>]

## I. INTRODUCTION

Since the pioneer work of Ono and collaborators<sup>1</sup> the manipulation of single magnetic domain wall (DW) in nanowires is a subject of intense research motivated by both its high potential for applications and its interest for fundamental physics. Among the different ways to stabilize a single DW in a magnetic track at a specific location, the use of a microfabricated notch is one of the most commonly used techniques. Nowadays, it is well recognized that the nature of the domain wall (i.e., transverse or vortex)<sup>2–5</sup> can have a strong influence on the depinning processes (assisted either by a magnetic field, spin polarized current, or by thermal excitations). Consequently, it is important to investigate in detail the influence of the notch on the DW structure. In this article, we report on the effect of a symmetric notch on the DW structure and its consequences on the depinning mechanism under an applied magnetic field. In a first step, we consider only one ferromagnetic layer and we show that, even for a defined type of DW, several stable states exist at the notch vicinity. In a second step, we take into account the presence of an additional ferromagnetic layer with magnetization fixed and aligned along the magnetic track in order to reproduce the conditions experienced by trapped DWs in a spin-valve stack. Again, in this case we find that several stable states exist.

In both systems considered we have studied the depinning mechanisms assisted by magnetic field and different depinning processes are unveiled. For the single thin film, it is shown that the process depends on the thickness of the film. For the spin-valve case (two ferromagnetic layers), two different mechanisms can occur for the same thickness, depending on the configuration of the hard layer. This last finding explains our experiments on DW depinning with a spin valve nanowire.

## II. EXPERIMENTAL RESULTS

We will consider here domain walls pinned by a notch in a spin-valve wire. The samples studied here are identical to

those presented in Refs. 6 and 7. The spin-valve film was grown by magnetron sputtering on a glass substrate with a structure (in nanometers) Ta(3)/Cu(2)/IrMn(6)/Co<sub>65</sub>Fe<sub>35</sub>(2.5)/Cu(3)/Co<sub>65</sub>Fe<sub>35</sub>(4)/Ni<sub>86</sub>Fe<sub>14</sub>(15)/Ru(6). The film exhibits an exchange bias field of the hard layer (IrMn/CoFe) of 120 mT and a reversal field of the free layer (CoFe/FeNi) of 1 mT. The GMR equals 3%. A 500 nm wide wire is patterned by ebeam lithography and Ar ion beam etching. A nucleation pad is situated at an extremity of the wire to inject a domain wall in it and a notch is positioned along the wire. The magnetic field is applied in the direction of the nanowire. At moderate fields (around 30 mT), the free layer magnetization saturates along the field, whereas the hard layer is not affected. Depending on the relative directions of the field and hard layer pinning direction, the configuration is either parallel (P) or antiparallel (AP). When the field is reversed and swept, the magnetization reversal of the free layer is initiated in the nucleation pad and is completed by propagation of the domain wall in the nanowire (the domain wall always propagates from the nucleation pad). Depending on the field sweep, the domain wall propagation therefore corresponds to P → AP or AP → P transitions. In the absence of hard layer, these two processes should be equivalent as they correspond to the same propagation of a head-to-head or tail-to-tail domain wall. During its propagation, the domain wall is trapped by the notch.

Figure 1(a) is a magnetic force microscopy image of a domain wall trapped by a notch. The nature of the observed contrast is typical from a vortex domain wall.<sup>8</sup> The contrast is also satisfactorily mimicked by the divergence of the magnetization obtained by micromagnetic simulation<sup>9</sup> (Figure 1(a)).

Figure 1(b) represents the typical evolution of the resistance (normalized) with the applied field. Starting from low field values (AP), a DW is injected and propagates to the notch resulting in an intermediate value of resistance. When the depinning field is reached (about 21 mT in the present case), the DW depins from the notch. The whole wire is thus

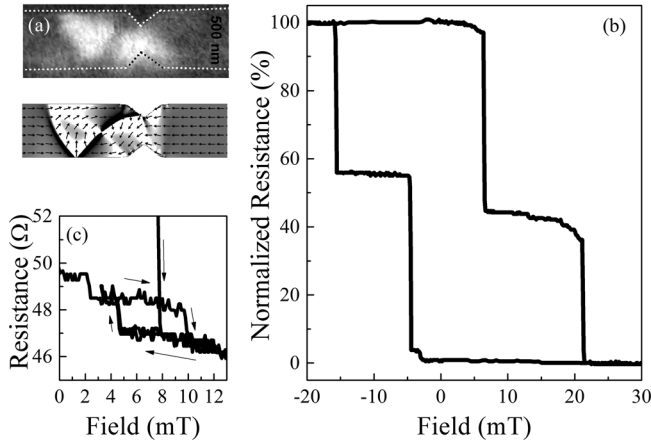


FIG. 1. (a) Magnetic force microscopy image of a magnetic domain wall trapped in the vicinity of a notch and divergence of the simulated micromagnetic configuration. (b) Normalized magnetoresistance of a typical device. (c) Minor loop highlighting the irreversible configuration changes for a pinned domain wall.

reversed leading to a minimum resistance (P state). For decreasing fields, the same behavior is observed but corresponds now to a  $P \rightarrow AP$  propagation (note that the direction of propagation is unchanged). The evolution of resistance as a function of field when the DW is pinned in the notch is different for  $P \rightarrow AP$  and  $AP \rightarrow P$ . Whereas, the resistance is almost constant for the  $P \rightarrow AP$  propagation, it exhibits a strong curvature for  $AP \rightarrow P$  propagation. We will see below that this difference in the "susceptibility" of the domain wall originates in differences in the nature of the domain wall in each case.

In some devices, two resistance levels are associated with the same pinned domain wall (Figure 1(c)). This corresponds to two different magnetic configurations with irreversible transitions between them. This kind of behavior is sometimes (i.e., for some devices) observed during the  $AP \rightarrow P$  domain wall propagation but has never been observed during the  $P \rightarrow AP$  propagation.

These two experimental facts suggest that there exist different possible magnetic configurations trapped in a notch and that these configurations are strongly affected by the

hard layer. However, before considering the effect of the hard layer, we first focus below on the different possible magnetic configurations in a single film.

### III. DOMAIN WALL CONFIGURATIONS AND DEPINNING IN A SINGLE FILM

Magnetic domain walls propagating in a stripe can exhibit different topologies. For in-plane magnetization, equilibrium configurations include vortex and transverse domain walls.<sup>10</sup> These equilibrium configurations are generally metastable states corresponding to local minima of the system energy. It has been shown that the nature of the domain wall is the determinant factor in the depinning process. Non-reproducibility of the nature of the injected domain wall has been shown to be a key ingredient in the stochastic behavior of domain wall depinning.<sup>5,7</sup>

Micromagnetic configurations of pinned DW are calculated using standard micromagnetic software OOMMF.<sup>9</sup> The geometry considered in this paper is shown in Figures 1 and 2. It consists in a 600 nm track containing a 300 nm constriction. Material parameters are representative of permalloy ( $860 \times 10^3$  A/m magnetization,  $13 \times 10^{-12}$  J/m exchange stiffness). As determined from full film measurements, a  $500 \text{ J/m}^3$  uniaxial anisotropy along the track direction has been included. All simulations are performed with a 2.5 nm cell size assuming uniform magnetization along the thickness of the film. It has been verified that the finite length of the simulated wire ( $4 \mu\text{m}$ ) has no influence on the computed magnetic configurations. In order to determine all the local energy minima, various initial conditions are systematically used.

At zero magnetic field, it appears that a surprisingly large number of different magnetic configurations are stable (Figure 2). Taking into account the different symmetries, 20 different stable configurations can be found. For vortex DWs, two types can be distinguished, depending on the position of the vortex core. Actually, the vortex core can be repelled outside the notch,  $V_a$  and  $V_f$ , or trapped in the constriction,  $V_c$  and  $V_d$  (Figure 2(b)). For transverse DWs, there exists only one type, represented as  $T_a$  and  $T_d$  in Figure 2(e). All the configurations are asymmetric, whereas the notch is symmetric.<sup>11</sup>

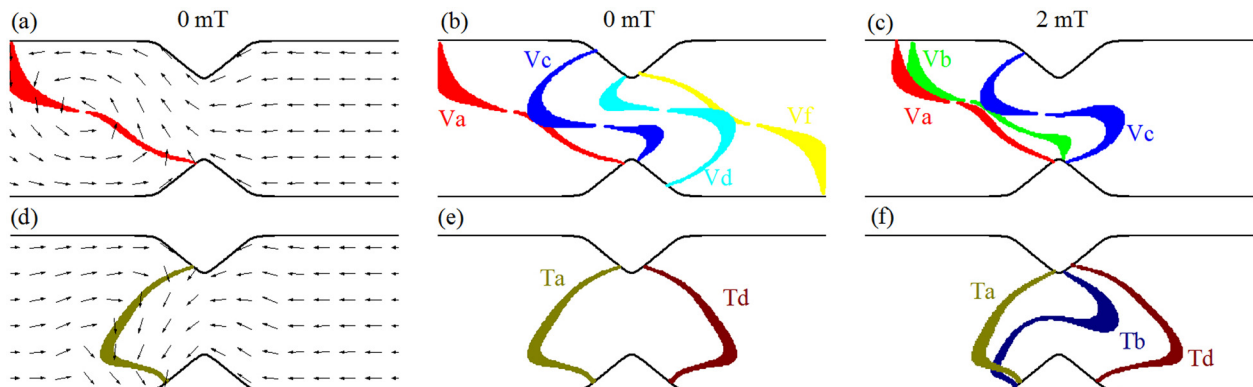


FIG. 2. Representations of the different vortex ((a)–(c)) and transverse ((d)–(f)) domain wall configuration within a 15 nm thick film. (a) and (d) Micromagnetic configuration of a vortex or transverse wall, the line figures of "the core" of the domain wall, defined as the region in which the magnetization is perpendicular to the stripe direction. (b) and (e) Different possible cores for the vortex or transverse domain wall at 0 mT. (c) Same at 2 mT.

Figure 3(a) represents the evolution of the energy of the domain wall as a function of the film thickness (for improved readability, the energy is divided by the square of the thickness). Similar to the case of a stripe without a notch,<sup>12</sup> for the large stripe width considered here, the vortex domain walls are energetically favored for a wide range of film thickness. We will thus concentrate on vortex walls in the following discussion (nevertheless most of the conclusions also hold for transverse domain walls).

In the presence of a magnetic field, the degeneracy between some configurations is lifted. Some configurations are no longer stable (the domain wall depins from the notch) and other configurations (not stable at zero field) are now possible. Figures 2(c) and 2(f) represent, respectively, vortex and transverse domain walls for a 2 mT applied field. For vortex DW's, the Vd and Vf configurations are no longer stable as their depinning field is below 2 mT. On the other hand, a new configuration, Vb, is now stable. This configuration is characterized by an overlap of the notch by the domain wall. A similar phenomenon occurs for transverse DW's with the Tb configuration (Figure 2(f)).

Figure 3(b) represents the field range of stability of Va and Vb configurations as a function of the film thickness. From this figure it appears that, starting from configuration Va, different depinning mechanisms can occur. In an intermediate thickness range (from 3.8 to 12.2 nm), the domain wall switches from configuration Va to configuration Vb (one extremity of the wall goes over the notch) and finally depins from the notch. By contrast, for thicknesses between 12.2 and 14.7 nm, the domain wall can depin directly from configuration Va, since Va is a metastable state and does not transit through the Vb configuration. These two depinning mechanisms are compared in Figure 4 for film thicknesses of 10 and 13 nm. For a 10 nm thickness (Fig. 4(a)) the domain wall switches from Va to Vb at 4 mT and then finally depins at 5 mT. We note that in the Vb configuration, the DW easily extends beyond the notch leading to a high "susceptibility." On the other hand for 13 nm (Fig. 4(b)), it depins directly from the Va configuration at a field of 6.1 mT. In both cases,

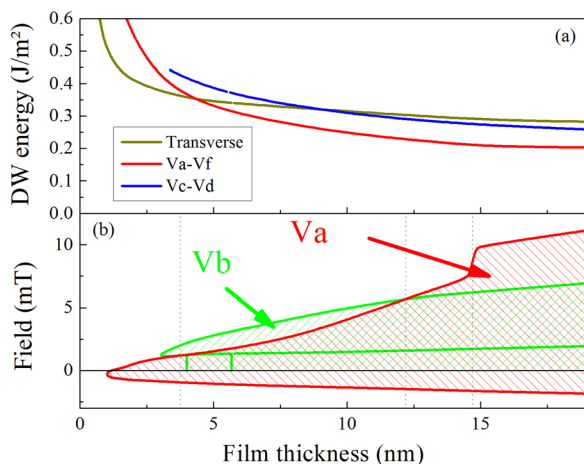


FIG. 3. (a) DW energy variation as a function of film thickness. The DW energy is divided by the square of the film thickness for an easier comparison of energies at a given thickness. (b) Field range of stability for the Va and Vb configurations as a function of film thickness.

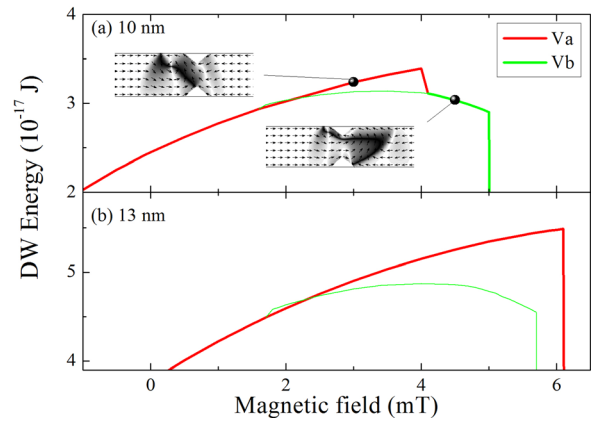


FIG. 4. Energy of the DW as a function of the applied field for two thicknesses of the film. (a) 10 nm, at 4 mT, the Va configuration is not stable anymore and the DW has to switch to Vb. (b) 13 nm, when the Va configuration is not stable anymore, the DW depins.

the domain wall depins from the notch in a transverse form (whereas this form presents a higher energy in this thickness range).

For low thicknesses (below 3.8 nm), the domain wall undergoes a transition from Va to a transverse configuration (Ta) before crossing the notch and finally depinning in a transverse form. At large thicknesses (above 14.7 nm), the depinning field from the Va configuration experiences a steep increase corresponding to a change in the depinning mechanism. As the depinning field increases, a new domain is nucleated in the vicinity of the notch. The domain wall thus becomes a 360° domain wall which is rapidly annihilated. This behavior has already been reported in the case of a square notch.<sup>13</sup>

#### IV. DOMAIN WALL CONFIGURATION AND DEPINNING IN SPIN-VALVES

After having detailed the different domain wall configurations and the different depinning mechanisms, we now considered the influence of the hard layer and the related stray magnetic fields. The interaction between the propagating DW and an additional ferromagnetic layer has several consequences<sup>14</sup> and it has been previously shown experimentally that the reference layer can influence considerably the depinning from a notch both for in-plane<sup>6</sup> and perpendicular<sup>15</sup> magnetization.

The reference layer stray field can be evaluated considering the micromagnetic configuration of the reference layer at the notch. We will consider here an exchange coupled 2.5 nm thick CoFe reference layer as in Ref. 6. The effect of the reference layer is thereafter evaluated considering the average stray field acting on the free layer in which the domain wall propagates. The influence of the free layer on the reference layer has been verified to be negligible compared to the 0.12 T bias field.

Considering the stray field from the notch, magnetic configurations are not drastically modified. The Vb configuration is still stable only in an intermediate field range but not in zero field. Figure 5 compares the magnetization and

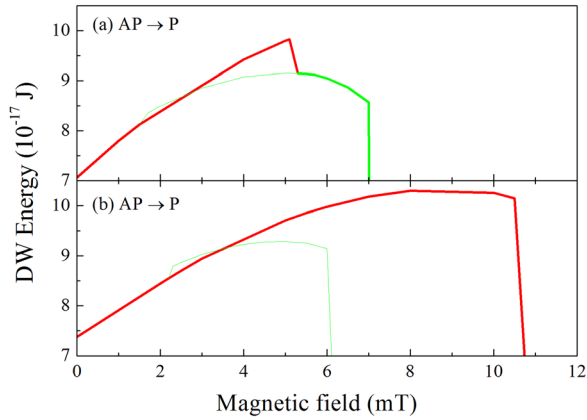


FIG. 5. Energy of the DW as a function of the applied field for a 19 nm thick film in the stray field of a hard layer. (a) AP  $\rightarrow$  P, at 5.3 mT, the Va configuration is no longer stable and the DW has to switch to Vb. (b) P  $\rightarrow$  AP, when the Va configuration is no longer stable and the DW depins.

energy of the Va and Vb configurations for the P  $\rightarrow$  AP and the AP  $\rightarrow$  P transitions for a 19 nm thick soft layer. These characteristics of each configuration are almost identical for the two transitions and therefore not significantly influenced by the stray field from the hard layer. The important difference is the stability of the configurations: for the P  $\rightarrow$  AP propagation, the behavior is similar to the single film; whereas for the AP  $\rightarrow$  P transition, the Va configuration is not as stable and the domain wall undergoes a transition from Va to Vb before depinning. This last behavior is also found in single films at much lower thicknesses.

The stray field from the hard layer being maximum at the center of the notch has only a small influence on the equilibrium configurations of both sides of the notch but strongly affect the barrier height between the configurations. The difference in the depinning mechanism for P  $\rightarrow$  AP and AP  $\rightarrow$  P propagation is highlighted in Figure 6 which represents the domain wall profile for different applied fields. For P  $\rightarrow$  AP

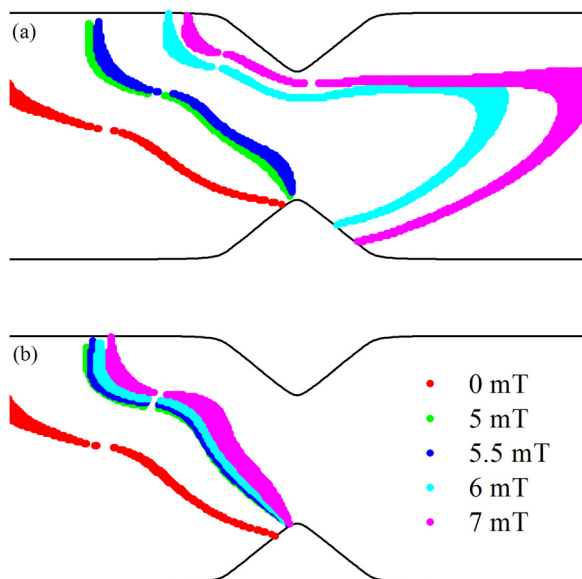


FIG. 6. Profiles of the vortex domain wall core for different applied fields for AP  $\rightarrow$  P (a) and P  $\rightarrow$  AP (b) propagation.

propagation, the domain wall is compressed on the notch (Va configuration) but for the AP  $\rightarrow$  P propagation the domain wall spans the notch by switching in the Vb configuration. In this last configuration, the domain wall extends progressively.

This behavior explains perfectly the experimental observations. For P  $\rightarrow$  AP propagation, as the domain wall is compressed on the notch, its configuration is mainly unchanged and gives rise to a flat plateau in the magnetoresistance. On the other hand, the switching to a Vb configuration during the AP  $\rightarrow$  P propagation, results in a "deformable" domain wall with a high magnetic susceptibility and consequently a curved plateau as the resistance varies with the applied field. The irreversible transitions sometimes observed during the AP  $\rightarrow$  P propagation could also be related to the switching from Va to Vb.

## V. CONCLUSIONS

In this article, we have reported experimental evidence of different behaviors of a pinned domain wall depending on its relative alignment with the hard layer of a spin valve (P  $\rightarrow$  AP or AP  $\rightarrow$  P propagation). To explain these observations, we have investigated numerically the different possible magnetic configurations possible for a domain wall pinned by a notch. Depending on the applied field, different configurations are possible and the depinning scenarios vary. Considering the presence of the hard layer of the spin valve and the related stray field at the notch, the depinning scenarios are drastically modified and can be different for P  $\rightarrow$  AP and AP  $\rightarrow$  P propagations.

The numerical simulations reproduce qualitatively the experimental observations and outline the influence of the hard layer on the depinning mechanism. As it is usually the case, the computed depinning fields are not quantitatively in agreement with experimental values. The influence of the microstructure and the presence of defects are likely one reason for the enhanced experimental depinning fields. Small differences between the experimental and simulated geometries can also lead to important differences in the depinning field estimation as it has been shown theoretically and experimentally that the depinning field is very sensitive to the exact geometry.<sup>16–18</sup> However, our main conclusions remain valid. First, the irreversible switching associated with the AP  $\rightarrow$  P propagation is due to the reduction of the barrier height by the stray field emanating from the hard layer, and this effect is independent of the exact nature of the configurations. Second, the different magnetic susceptibilities observed for P  $\rightarrow$  AP and AP  $\rightarrow$  P propagation are systematic from device to device and are therefore not linked to some particular defects and are really an indication of different magnetic configurations.

The phenomena we have highlighted in this article are not specific to our geometry and can be similarly encountered in smaller stripes and other kind of pinning centers. The presence of different magnetic configurations (not only related to DW nature or chirality) must therefore be considered as it can have significant influence on the depinning process and can explain complex stochastic behaviors.

## ACKNOWLEDGMENTS

The work presented in this article was partly supported by La Région Lorraine. J.B. acknowledges support from CONACYT. The authors acknowledge G. Lengaigne for technical assistance.

- <sup>1</sup>T. Ono, H. Miyajima, K. Shigeto, and T. Shinjo, *Appl. Phys. Lett.* **72**, 1116 (1998).
- <sup>2</sup>M. Kläui, C. A. F. Vaz, J. Rothman, J. A. C. Bland, W. Wernsdorfer, G. Faini, and E. Cambril, *Phys. Rev. Lett.* **90**, 097202 (2003).
- <sup>3</sup>A. Thiaville and Y. Nakatani, *Spin Dynamics in Confined Magnetic Structures III*, Topics in Applied Physics Vol. 101, edited by B. Hillebrands and A. Thiaville (Springer, Berlin, 2006), p. 161.
- <sup>4</sup>L. K. Bogart, D. Atkinson, K. O'Shea, D. McGrouther, and S. McVitie, *Phys. Rev. B* **79**, 054414 (2009).
- <sup>5</sup>J. Akerman, M. Muñoz, M. Maicas, and J. L. Prieto, *Phys. Rev. B* **82**, 064426 (2010).
- <sup>6</sup>J. Briones, F. Montaigne, D. Lacour, M. Hehn, M. J. Carey, and J. R. Childress, *Appl. Phys. Lett.* **92**, 032508 (2008).
- <sup>7</sup>J. Briones, F. Montaigne, M. Hehn, D. Lacour, J. R. Childress, and M. J. Carey, *Phys. Rev. B* **83**, 060401 (2011).
- <sup>8</sup>R. Moriya, L. Thomas, M. Hayashi, Y. B. Bazaliy, C. Rettner, and S. S. P. Parkin, *Nat. Phys.* **4**, 368–372 (2008).
- <sup>9</sup>M. J. Donahue and D. G. Porter, OOMMF User's Guide Version 1.0, National Institute of Standards and Technology, Report No. NISTIR 6376 1999.
- <sup>10</sup>R. D. McMichael and M. J. Donahue, *IEEE Trans. Magn.* **33**, 4167–4169 (1997).
- <sup>11</sup>D. Djuhana, H.-G. Piao, S.-H. Lee, D.-H. Kim, S.-M. Ahn, and S.-B. Choe, *Appl. Phys. Lett.* **97**, 022511 (2010).
- <sup>12</sup>Y. Nakatani, A. Thiaville, and J. Miltat, *J. Magn. Magn. Mater.* **290**, 750 (2005).
- <sup>13</sup>J. Akerman, M. Muñoz, M. Maicas, and J. L. Prieto, *J. Appl. Phys.* **115**, 183909 (2014).
- <sup>14</sup>N. Rougemaille, V. Uhlir, O. Fruchart, S. Pizzini, J. Vogel, and J. C. Toussaint, *Appl. Phys. Lett.* **100**, 172404 (2012).
- <sup>15</sup>S. Park, N. M. Nguyen, C. Burrowes, E. E. Fullerton, C. Chappert, L. Prejebeanu, F. Garcia-Sanchez, and D. Ravelosona, *Appl. Phys. Lett.* **98**, 232512 (2011).
- <sup>16</sup>M.-Y. Im, L. Bocklage, P. Fischer, and G. Meier, *Phys. Rev. Lett.* **102**, 147204 (2009).
- <sup>17</sup>H. Y. Yuan and X. R. Wang, *Phys. Rev. B* **89**, 054423 (2014).
- <sup>18</sup>S. Goolaup, S. C. Low, M. Chandra Sekhar, and W. S. Lew, *J. Phys.: Conf. Ser.* **266**, 012079 (2011).